THE JOURNAL OF PHYSICAL CHEMISTRY B

ARTICLE

pubs.acs.org/JPCB

Spiral Superstructures of Amyloid-Like Fibrils of Polyglutamic Acid: An Infrared Absorption and Vibrational Circular Dichroism Study

Aleksandra Fulara,[†] Ahmed Lakhani,[‡] Sławomir Wójcik,[†] Hanna Nieznańska,[§] Timothy A. Keiderling,*[,‡] and Wojciech Dzwolak*[,†]

[†]Department of Chemistry, University of Warsaw, Pasteura 1, 02-093 Warsaw, Poland

[‡]Department of Chemistry, University of Illinois at Chicago, 845 West Taylor Street (m/c 111), Chicago, Illinois 60607-7061, United States

[§]Nencki Institute of Experimental Biology, Polish Academy of Sciences, Pasteura 3, 02-093 Warsaw, Poland

Supporting Information

ABSTRACT: Amyloid fibrils, which are often associated with certain degenerative disorders, reveal a number of intriguing spectral properties. However, the relationship between the structure of fibrils and their optical traits remains poorly understood. Poly(L-glutamic) acid is a model polypeptide shown recently to form amyloid-like fibrils with an atypical infrared amide I′ band at 1595 cm^{-1}, which has been attributed to the presence of bifurcated hydrogen bonds coupling C═O and N—D groups of the main chains to glutamate side chains. Here we show that this unusual amide I′ band is observed only for fibrils grown from pure enantiomers of the polypeptide, whereas fibrils precipitating from equimolar mixtures of poly(L-glutamic) and poly(D-glutamic) acids have amide I′ bands at 1684 and 1612 cm^{-1}, which are indicative of a typical intermolecular antiparallel β-sheet. Pure enantiomers of polyglutamic acid form spirally twisted superstructures whose handedness is correlated to the amino acid chirality, while fibrils prepared from the racemate do not form scanning electron microscopy (SEM)-detectable mesoscopically ordered structures. Vibrational circular dichroism (VCD) spectra of β-aggregates prepared from mixtures of all L- or D-polyglutamic acid in varying ratios indicate that the enhancement of VCD intensity correlates with the presence of the twisted superstructures. Our results demonstrate that both IR absorption and enhanced VCD are sensitive to subtle packing defects taking place within the compact structure of amyloid fibrils.

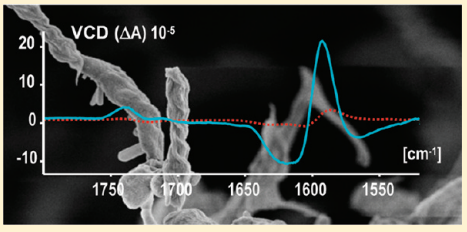

INTRODUCTION

In vivo deposits of amyloid fibrils have long been associated with several degenerative disorders such as Alzheimer's disease.[1] Despite recent progress,[2,3] the current understanding of amyloid structure and the dynamics leading to its formation remains unsatisfactory. The cross-β assembly of stacks of H-bonded β-strands that form the core of most amyloid fibrils have distinct tinctorial and optical properties from those of β-sheets present in globular proteins. Some of the most fascinating yet least understood optical traits of amyloid fibrils are their strong chiroptical properties, such as the powerful enhancement of circular dichroism detected in both the electronic[4,5] and the vibrational spectral regions.[6] Our previous studies have shown that the origins of the strong electronic circular dichroism (ECD) of insulin amyloid fibrils are superstructural, while its sign (negative or positive) may, under certain conditions, be elected randomly despite the uniform L-chirality of the protein's amino acid residues.[4,5] In recent work on insulin amyloid, Kurouski and colleagues were able to link opposite signs of vibrational circular dichroism (VCD) signal to variants of fibrils with opposite senses of helical twist as detected using atomic force microscopy (AFM).[7]

Poly(L-glutamic) acid (PLGA) is a model homopolypeptide known to adopt, depending on pH and temperature, different structures including β-sheet-rich amyloid-like fibrils.[8,26] Itoh et al. showed that, at an appropriately low pH and high temperature, PLGA forms two distinct types of antiparallel β-sheet conformation, termed β_1 and β_2, with pronounced spectral differences in the amide I/I′ vibrational region.[9] While the β_1 structure has its amide I′ band split into strong (~1612 cm^{-1}) and weak (>1680 cm^{-1}) components, which are typically associated with the formation of intermolecular antiparallel β-sheets, the β_2 structure has its intense amide I′ component shifted below 1600 cm^{-1}, a position not observed in the infrared spectra of proteins. Despite these spectral dissimilarities, X-ray diffraction data suggested that both β_1 and β_2 structures are quite similar, with the latter being more compressed in the direction perpendicular to the β-sheet plane.[9] In a recent Fourier transform infrared (FT-IR) study, we have proposed that the tight intersheet packing characteristic of the β_2 aggregate facilitates the formation of unusual three-center hydrogen bonds involving bifurcated main chain carbonyl acceptors and main chain NH (ND), as well as side chain −COOH (−COOD) donors.[10]

Received: July 3, 2011
Revised: August 12, 2011
Published: August 15, 2011

According to this hypothesis, the formation of bifurcated hydrogen bonds between strands of the β-sheets would reduce the amide C═O bond strength and consequently shift the amide I (amide I′) frequency down. The coupling of dipoles in an ordered β-sheet structure would still dominate the IR band shape,[13] so that the strong features below 1600 cm^{-1} would correspond to the out-of-phase (in the strand) component of the exciton band. The high frequency mode would also shift, since it is an exciton component of the coupled reduced frequency oscillators, but its assignment is less clear and will be addressed here. Both the H-bond and the coupling interactions underlie the observed spectral features of β_2 fibrils.

β_2 PLGA fibrils are an intriguing example of how periodic, tightly packed structures composed of aligned polypeptide chains foster interactions that are normally rare in "biological" β-sheets, leading to unusual physicochemical properties. The initial goal of this work was to study how the disruption of these interactions, by inducing packing defects in mixed aggregates containing both PLGA and poly(D-glutamic) acid (PDGA), would affect their optical properties. We have employed VCD as a complementary tool to FT-IR spectroscopy, as it can provide added insight for protein conformational characterization.[6,7,11,12] Furthermore, developing such a data set will provide an experimental basis for future tests of theoretical methods for interpretation of VCD spectra of stacked β-sheet structures in terms of both conformation and superstructure.[13,14]

Since X-ray diffraction and solid state NMR methods require that samples are relatively defect-free, there is a need for complementary optical and microscopic approaches capable of probing subtle packing imperfections within fibrils, as these may contribute to eventually understanding the variable biological activity of amyloid fibrils in vivo.[25]

MATERIALS AND METHODS

Samples. Generally, freshly prepared aggregates were used for subsequent FT-IR/VCD/TEM/SEM measurements. PLGA and PDGA (as sodium salts) (molecular weight (MW), 15−50 kDa) were purchased from Sigma. Branching of homopolypeptide main chains, which may occur in commercial preparations of PLGA/PDGA, is undesirable, as it prevents proper folding and packing of polypeptide structures. The lots of PLGA and PDGA used in this work were 096K5103 and 097H5907, respectively.

Unless indicated otherwise, the typical preparative routine of PLGA/PDGA β-sheet aggregates consisted of dissolving sodium salt(s) of polyglutamic acid in D_2O at 1 wt % concentration and subsequent acidification with diluted DCl to pD $\sim$ 4.1 (uncorrected for isotopic effects), as described earlier.[10] For all mixed (PLGA and PDGA) aggregates, polyglutamic acid solutions of each enantiomer were prepared at neutral pD, and then the desired proportions were mixed and vortexed for 30 min before the pD adjustment. The preparation of stock fibrils involved incubating the freshly acidified polypeptide samples for 44 or 48 h at 65 °C. Since the predisposition of homopolypeptides to aggregation strongly depends on molecular weight,[15] the MW of polyglutamic acid was characterized using size exclusion chromatography (SEC), which has been described in detail in the Supporting Information. D_2O and DCl were obtained from ARMAR Chemicals, Switzerland, or Cambridge Isotopes, while ThT was from Sigma.

FT-IR Spectroscopy. For most FT-IR measurements, a CaF_2 transmission cell equipped with 25 μm Teflon spacers was used. FT-IR spectra were collected on a Nicolet NEXUS FT-IR spectrometer equipped with a liquid nitrogen-cooled MCT detector at 2 cm^{-1} resolution. The chiral mixed samples were also measured in a homemade cell with a 50 μm spacer on a Bruker Vertex 80 spectrometer with a DTGS detector at 4 cm^{-1} resolution. Typically, for a single spectrum 256 interferograms were coadded, and the sample chamber was continuously purged with dry air. From each sample's spectrum, corresponding buffer and water vapor spectra were subtracted. Since concentrations for such fibrilized samples are not well-characterized and they tended to precipitate over time, the spectra were normalized according to the integrated intensity of the amide I band or the highest single peak in the spectral region. Data processing was performed with GRAMS software (ThermoNicolet, USA). All further experimental details were the same as specified earlier.[10,16]

Vibrational Circular Dichroism. Spectra were measured on both freshly prepared samples and equilibrated (one week) samples in the same cells used for FTIR using a homemade dispersive instrument separately described in detail.[17] Briefly, it consists of a 0.3 m monochromator (Acton Research Corporation, SpectraPro 2300i), C-Rod source, wire grid polarizer, 57 kHz CaF_2 modulator (Hinds International) and a narrow-band, liquid-nitrogen-cooled MCT detector (Infrared Assoc.). The signals were separated and independently digitized for the transmission and modulation intensity, which were then ratioed to yield the raw circular dichroism (CD) spectra by use of a computer programmed in LabView that also controls the data collection. VCD measurements were carried out with 12 cm^{-1} spectral resolution and accumulated as the average of four scans. Baselines were partially corrected by subtraction of an identically collected spectrum of a cell containing only D_2O. Additional spectra were obtained for precipitated films to provide a comparison and further enhancement of VCD intensity. These were checked for orientational dependence, which was found to be negligible.

ThT Fluorescence Measurements. ThT fluorescence measurements were carried out under typical conditions.[10] Namely, 0.3 wt % aqueous stock solution of ThT was added to 10-times diluted stock PLGA sample (pH approximately 4) to the final concentration of the dye 25 μM. The fluorescence of ThT-stained aggregates was excited at 450 nm and measured using a AMINCO Bowman Series 2 luminescence spectrometer.

Transmission Electron Microscopy. For TEM observations copper grids (400 mesh) covered with collodion (SPI Supplies, West Chester, PA, USA) and carbon were used. A 10 μL sample (1 mg/mL) was applied to a grid for 40 s and then negatively stained for 25 s with 2 wt % uranyl acetate (SPI Supplies, West Chester, PA, USA). Grids were dried at room temperature and examined using a JEM 1400 electron microscope (JEOL Co., Japan 2008) with a high resolution digital camera (CCD MORADA, SiS-Olympus, Germany).

Scanning Electron Microscopy. For SEM, droplets of aqueous suspensions of aggregates were deposited on silicon wafers and dried under vacuum (approximately 0.05 mbar) at room temperature. Films of fibrils were sputtered with approximately 40 nm thick layers of Au/Pd alloy before SEM images were collected on a Zeiss Leo 1530 microscope.

Raman Measurements. Polypeptide films were deposited onto microscopic glass slides (from Menzel-Gläser, Germany) and allowed to dry. All Raman measurements in 180° backscattering mode were carried out using a Thermo Scientific Nicolet 8700

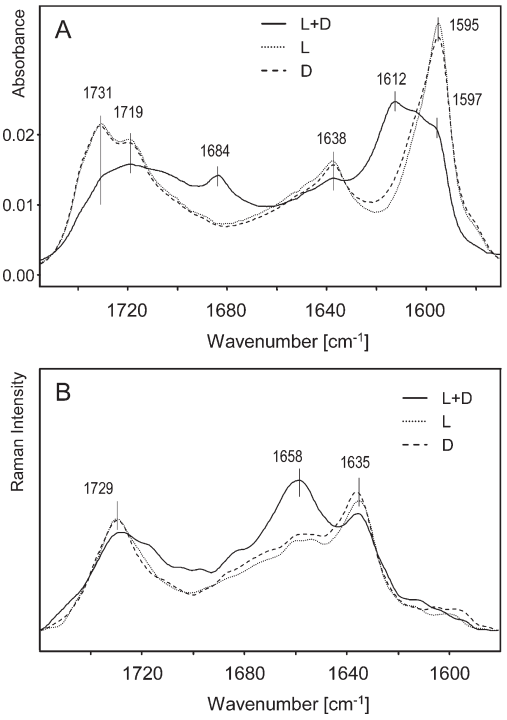

Figure 1. (A) FT-IR absorption spectra of suspensions of aggregates precipitating upon prolonged incubation at 65 °C of acidified (pD 4.1) 1 wt % solutions in D_2O, measured in a 50 μm path cell, of PLGA (dotted line), PDGA (dashed line), and their equimolar mixture (solid line). (B) Corresponding FT-Raman spectra of dry films of aggregates.

spectrometer equipped with a Raman NXR FT-Raman module with MicroStage microscope, a thermoelectrically cooled InGaAs detector, and a Nd:YVO_4 laser operating at 1064 nm and 0.5 W power. Typically, 1024 interferograms of 6 cm^{-1} resolution were coadded for a single Raman spectrum.

RESULTS AND DISCUSSION

FT-IR and Raman spectra of cross-strand hydrogen-bonded β-structured aggregates from PLGA, PDGA, and their equimolar racemic mixture are juxtaposed in Figure 1. Upon prolonged incubation at low pD and high temperature, enantiomerically pure chains of polyglutamic acid convert into insoluble precipitates. Their IR spectra have an unusually low frequency, with an intense amide I′ component that is downshifted to 1595 cm^{-1} and a weaker band at 1638 cm^{-1} with only very weak absorbance to higher frequency in the L- or D-only fibril spectra (Figure 1A, dashed and dotted lines). A strongly split pair of exciton components is typical of an antiparallel β-sheet conformation, but these are normally seen at higher frequencies, for example, 1693 and 1624 cm^{-1} for β-polyglutamates.[27] In the Raman spectra of deuterated L-only or D-only samples, an intense band appears at 1635 cm^{-1} with weaker features to a higher frequency (~1650−60 cm^{-1}, Figure 1B). Previously, we hypothesized that the strongly compressed β_2 structure is stabilized by intersheet bifurcated hydrogen bonds, leading to a reduction in frequency for the amide C═O oscillators, which is then reflected in the lower frequency of the exciton split component.[10] While it is possible that the 1638 and 1595 cm^{-1} bands form a shifted pair of IR-active, exciton-split components for an antiparallel β-sheet structure, that would imply a significant decrease in the exciton coupling and make the Raman (Figure 1B) difficult to explain. Raman spectra of a well-formed antiparallel β-sheet should have an intense in-phase (symmetrical) mode whose frequency would normally lie between those of the split IR active components. Our preliminary test calculations indicate that twisting and variation in size do not affect this basic qualitative pattern for the IR and Raman spectra of antiparallel structures (V. Profant, J. Kubelka, T. A. Keiderling, unpublished results). By contrast this is just the pattern one would see for parallel sheets, but the structural evidence of Itoh et al.[9] argue against such a model for this transformation. Alternatively one must assume that the symmetry is reduced in the β_2 form of PLGA, so that the Raman allowed band gains intensity in the IR, which is a pattern we can see in our calculational models for short sheet segments, and that the weaker IR exciton component is perhaps part of the shoulder on the high frequency side of the 1635 cm^{-1} band. The altered distribution of intensities and dispersion of frequencies, centered on a lower isolated oscillator frequency, may result from change in dipole strength or orientation in the bifurcated H-bonded C═O oscillators, although the former is not evident in our spectra. The characteristic pair of bands at 1731/1719 cm^{-1} is assigned to stretching vibrations of Glu−COOD groups in β_2 fibrils.

By contrast, the racemic aggregate that precipitates upon heating the acidified mixture of PLGA and PDGA has IR spectral features that are reminiscent of a typical intermolecular antiparallel β-sheet (Figure 1A), such as observed in amorphous aggregates of denatured proteins, or formed by several homopolypeptides.[8] The changes are evidenced by a decrease in the intensities of the 1595 and 1638 cm^{-1} bands, while new peaks at 1612 and 1684 cm^{-1} emerge. The −COOD band above 1700 cm^{-1} is broader and somewhat lower in frequency, no longer split and narrow, suggesting the presence of a less structured environment for repeated Glu side chains. The corresponding Raman spectral changes for the mixed enantiomer sample, having the primary amide I band centered around 1658 cm^{-1}, also reflect a reversion to the normal pattern (Figures 1B). Both the FT-IR and the Raman data suggest that the racemic aggregates are structurally inhomogeneous since they retain significant spectral characteristics of the β_2 conformer although now dominated by the β_1 conformer.

Several previous studies have been devoted to self-assembling interactions between polypeptides of opposite chiral symmetries. We have shown earlier that, in mixed solutions of poly(L-lysine) and poly(D-lysine), the formation of racemic, rather than enantiomerically pure, fibrillar β-aggregates is preferred due to reduced thermodynamic frustration at the polypeptide/water interphase.[20] In the case of polylysine aggregates, the position of the amide I′ band of the racemic β-sheet is blue-shifted compared to fibrils formed from separate enantiomers which could be due to change in interstrand hydrogen bonding but more likely arises from disrupted or less extended exciton coupling due to disorder in packing. Similarly, the substitution of poly(L-lysine) with poly(D-lysine) in electrostatically stabilized multilayered complexes with PLGA blue-shifts the amide I band, while the overall β-sheet conformation is maintained.[21] On the other hand, in the case of polyglutamic acid, the consequences of racemization in the β-sheet structure are more pronounced. The unique hydrogen bonding pattern and its influence over the amide I band no longer hold when possible L/D packing defects appear in the aggregate.

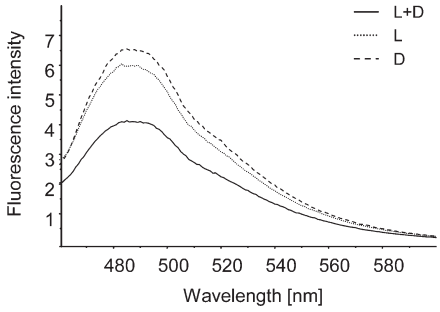

Figure 2. Fluorescence emission of the three different types of polyglutamic acid aggregates stained with ThT.

To assess whether these localized perturbations affect the higher order structures of the aggregates, we used the fluorescence of ThT, a fluorophore that can be used to sense fibril formation, and electron microscopy. Quantum yields of ThT fluorescence may increase by up to 3 orders of magnitude when bound to amyloid fibrils, but not amorphous β-sheets. ThT molecules, when docking onto a fibrous scaffold, are prevented from intramolecular rotation and self-quenching of fluorescence through a mechanism termed the "twisted internal charge transfer".[22] Because, unlike amyloid fibrils, native and denaturated states do not provide sufficiently rigid environment capable of freezing rotation of bound ThT molecules, the dye has become a selective probe of amyloid deposits.[23] As shown in Figure 2, the ThT fluorescence intensity is somewhat lower for racemic aggregate than for L- or D-only fibrils but is still quite intense and thus indicative of fibril formation. One obvious factor, namely, an incomplete conversion of the polypeptide into the β-sheet conformation, is doubtful, as all of the observed spectral components of the amide I band correspond to a predominantly extended (β-sheet) structure (whether with bifurcated HBs or not).

We have examined morphology of the aggregates using TEM with negative staining. The images shown in panels A, B, and C of Figure 3 provide strong evidence that all three types of polyglutamic acid aggregates are fibrillar. However, the racemate consists of loosely aggregated protofilaments (Figure 3C), while single enantiomer polyglutamic acid forms fibrils clustered in large twisted bunches approximately 200 nm thick, with individual fibrils being 5−10 nm in diameter. Although SEM lacks the high resolution of TEM, needed for detection of single amyloid fibrils, it is better suited for morphological analysis of larger superstructures. SEM images in Figure 3 (panels D−F) confirm the presence of twisted bunches of fibrils in enantiomerically pure samples (the superstructural entities may appear a bit thicker in SEM, which to a degree is caused by thick layers of sputtered Au/Pd alloy). Importantly, the fibrils appear to form elegant spiral superstructures with their handedness coinciding with the chirality of the polypeptide chain (i.e., PLGA forms left-handed, and PDGA right-handed spirals). These helical entities are absent in the SEM images of the racemate (Figure 3F), which on this superstructural scale (micrometer) lacks a defined morphology. The small crystals scattered around the polypeptide aggregates in Figure 3 are likely to be traces of noneluted salts.

Coupling the fluorescence and EM observations, it appears that the intensity of ThT emission increases when the dye binds to twisted amyloid superstructures rather than to lose fibrils. This scenario is in accordance with recent studies pointing out that the quantum yield of fluorescence strongly depends on the angle of twisting of "frozen" ThT molecules,[22] while the angle itself is thought to be imprinted by the local twist of fluorophore-binding β-sheets.[24] Thus, we suggest that the relatively high extrinsic fluorescence emission from L- and D-only aggregates of polyglutamic acid is yet another consequence of their superstructural organization.

Applications of VCD spectroscopy for a comparison of pure (from PLGA or PDGA only) and mixed (PLGA + PDGA) aggregates can be constrained by the lack of optical activity of the latter. As the ratio of L- and D-enantiomers becomes equivalent, the mixture becomes a pseudo-racemate, and its VCD signal diminishes down to our detection limits. On the other hand, by titrating PLGA with PDGA, we could monitor the progressive effect of disruption of the homopolymer interaction by its enantiomeric complement and the corresponding changes in the aggregate conformation. As compared to the IR, the VCD changes were dramatic for mixing in small amounts of the opposite enantiomer, as shown in Figure 5. These VCD (Figure 5A,C,D) and corresponding IR (Figure 5B) data were obtained for freshly prepared fibrils as suspensions in aqueous (acidic) solutions. For comparison, VCD were also measured for films prepared by depositing the aggregated acidified PLGA on a CaF_2 window. These spectra were more intense and evidenced no orientational dependence which would indicate any potential artifacts due to anisotropy (see the Supporting Information, Figure S1). The film VCD had qualitatively the same shape as did the fibril VCD but developed a broadened negative to lower frequency from the main amide I feature and had a mostly negative broad band associated with the −COOD. It is important to realize that the commercially available PLGA and PDGA samples accessible to us were not fully equivalent, as witnessed by the difference in their VCD spectra which are approximately mirror image in shape but not in intensity (Figure 4). In particular the PDGA polymer has VCD with a much lower intensity in these fibrillar states than does the PLGA. The difference in D- and L-isomers is basically not detectable in the FT-IR or Raman spectra (Figure 1) but in VCD results in significant intensity variation, suggesting it involves a structural variation that does not alter the FF (force field) on a local (near neighbor) length scale but does change the aggregate coupled, longer-range interaction between the oscillators. We also note that the kinetics of formation of the β-sheet conformation for PLGA and PDGA were distinct (data not shown). This behavior presumably derives from differences in the extent of polymerization and distribution of molecular weights and/or branching in the two samples. Thus we must analyze the VCD spectra of these two forms and their various combinations primarily on a qualitative basis.

The PLGA VCD spectra (Figure 5A) are dominated by an intense positive then negative couplet (low to high, with a weak and broad negative to lower wavenumber) centered on the amide I absorbance at ∼1590 cm^{-1} for PLGA. A second somewhat unusual feature is the positive couplet associated with the −COOD modes. That it has significant VCD with a distinctive couplet shape strongly suggests the side chains form an ordered array, at least over a short range. While the amide I shape is mirrored in the PDGA spectrum, the −COOD band may be shifted and altered in shape, which would suggest that the ordering of side chains is either not to the same extent or is differently configured in our PDGA samples. Alternatively it could indicate that the −COOD spectrum is a three-component

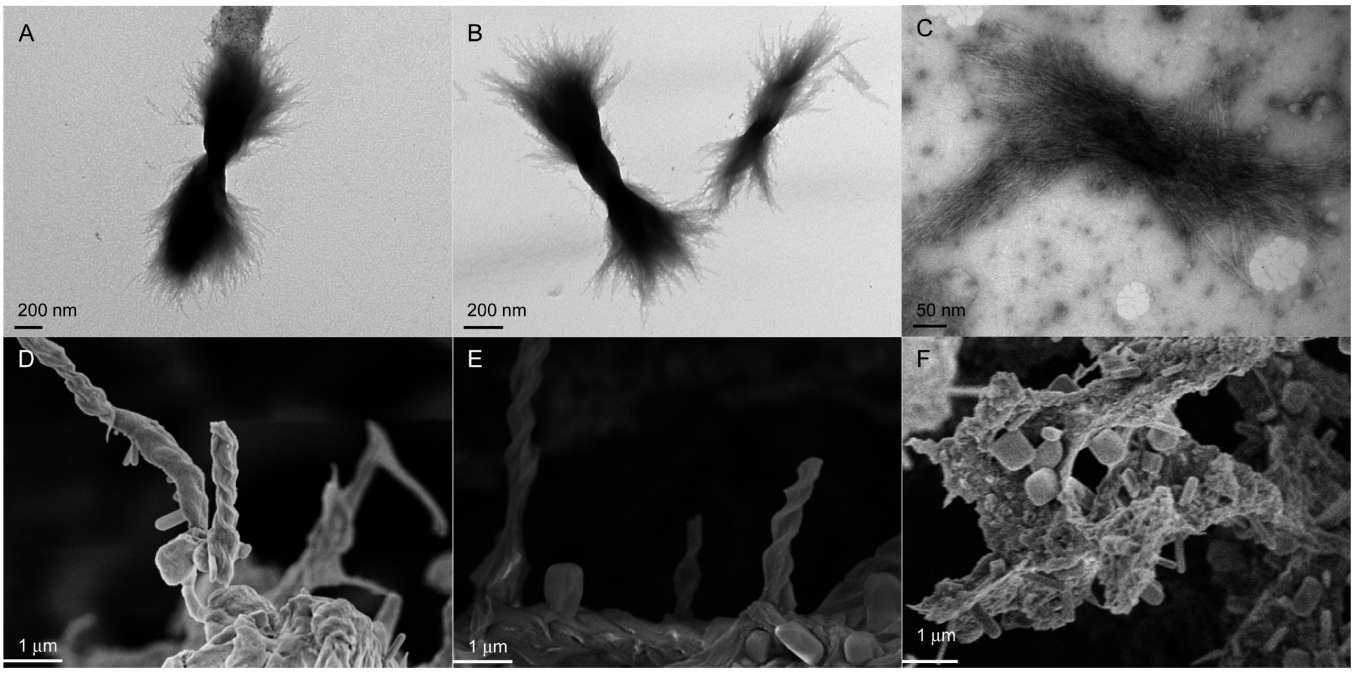

Figure 3. TEM (A−C) and SEM (D−F) images of the aggregates precipitating from acidified solutions of PLGA (A, D), PDGA (B, E), and an equimolar mixture of PLGA/PDGA (C, F) after a 44 h long incubation at 65 °C.

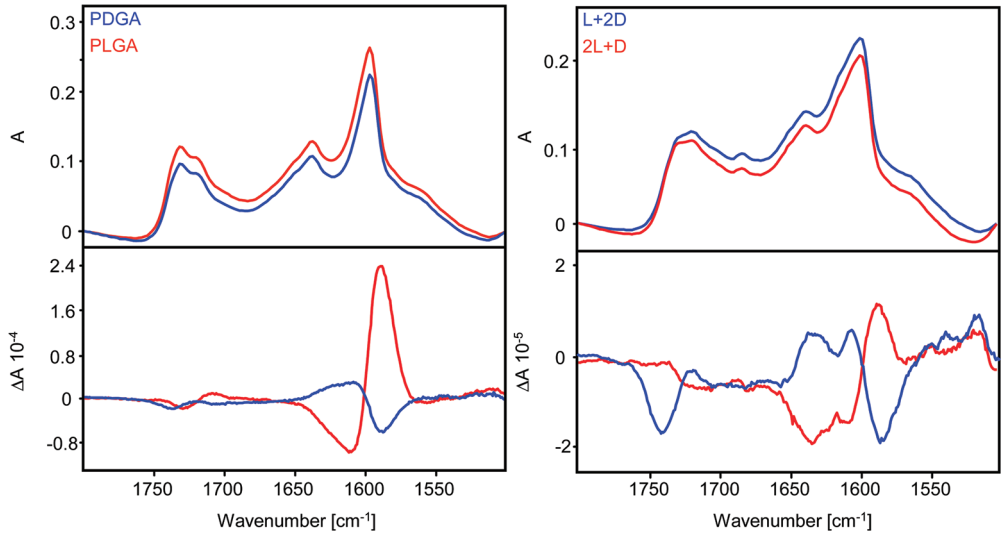

Figure 4. FT-IR (top) and VCD (bottom) spectra of suspensions (in acidified D_2O) of aggregates of PLGA and PDGA and their mixtures at a 1:2/2:1 molar ratio.

band (+,−,+) for PLGA, as brought out by an overlap of the two (Figure 4).

Interestingly, even only a one-fifth molar ratio (4 L+D) of PDGA added to PLGA causes a significant change in the band shape (Figure 5A,C), while changes in the corresponding IR spectra are small (Figure 5B). More importantly, this is associated with a dramatic loss in PLGA VCD intensity (Figure 5A). At 20% PDGA the large PLGA couplet at ∼1590 and 1620 cm^{-1} virtually collapses, and a new amide I′ VCD feature grows in at ∼1630 cm^{-1} next to the PLGA remnant VCD. The new band shape suggests the formation of a VCD component centered on the 1638 cm^{-1} absorbance but overlapped by the negative component of the PLGA VCD couplet, causing an apparent frequency shift. Surprisingly the −COOD couplet reverses sign in the mixed aggregate. As more PDGA is added to PLGA, the shape of the VCD is basically maintained, but the intensity decreases, so that at 33% PDGA (2 L:1D − Figure 5D) the amide I′ intensity is less than half of that at 25% (3 L:1D), and at 40% (1.5 L:1D) PDGA it is reduced even further. For the latter, the −COOD VCD is only slightly above the instrumental baseline.

The scale of pronounced decrease of VCD amplitude upon doping PLGA with PDGA (Figure 5A) cannot be explained by

dx.doi.org/10.1021/jp206271e |J. Phys. Chem. B 2011, 115, 11010–11016

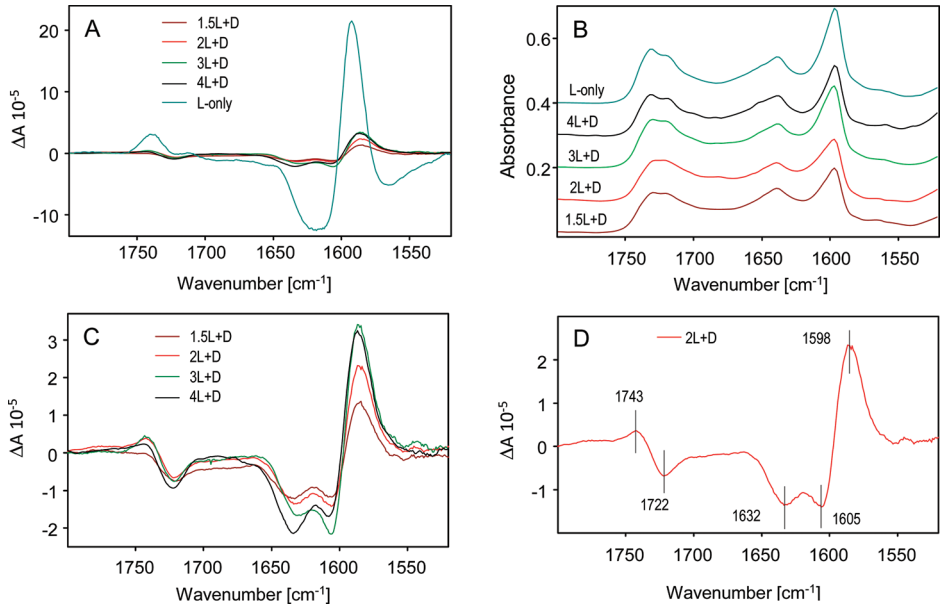

Figure 5. Effect of the changing L/D ratio on VCD (A) and corresponding original IR (B) spectra of PLGA/PDGA aggregates. Suspended fibrillar samples prepared as in Figure 1 and measured in a 25 μm path cell. In panel C, VCD spectra of only the L/D mixed aggregates are expanded. Peak positions in the spectrum of 2 L:1D (33% e.e.) aggregate are indicated in panel D.

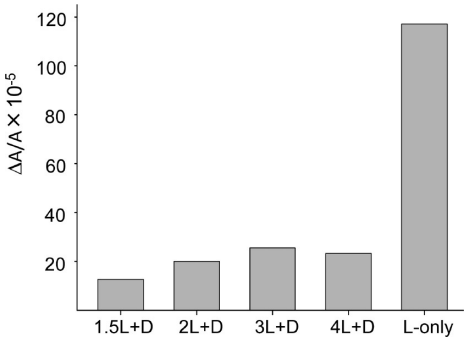

Figure 6. Dependence of normalized (divided by the corresponding intensity of amide I′ IR absorption) amplitudes of the VCD signal on the composition of the aggregate. Exact values are listed in Table 1 in the Supporting Information.

trivial effects of enantiomeric dilution and must originate in the loss of superstructural order in spiral aggregates, as evident in the SEM data (Figure 3). Plotting VCD amplitudes normalized according to the corresponding amide I′ band absorptions for different L/D ratios (Figure 6) suggests that the VCD enhancement is maintained only when the aggregate's structure is unperturbed by intrusions of chains with the opposite chirality. This behavior can be correlated with the observations above from TEM and SEM structures of the fibril (pure enantiomer) and mixed aggregate (L,D) structures.

While earlier theoretical works have suggested that twisting the β-strands may enhance the measurable VCD[13,14,18,19] and enhanced VCD have been detected in amyloid fibrils by other groups,[6,7] our study suggests that the spiral superstructures formed from PLGA fibrils may accommodate twisted (and therefore mechanically strained) strands into stable microarchitectures which give strong VCD. Chiroptical methods may thus provide insight into the structure of these protein assemblies that goes beyond the scale of conformation of polypeptide chains. These results suggest that VCD, normally viewed as a local probe of conformation, can become sensitive to longer-range spatial arrangement of protein folds.

In light of the results of this study, VCD spectroscopy can be seen as a sensitive tool for studying packing defects in fibrils, such as are likely common features of in vivo grown amyloid fibrils. Such discontinuity sites within the amyloid lattice (caused either by partial protein degradation or inclusion of small molecules and ions) may affect biological activity (e.g., toxicity) of fibrils and are of interest for further research.

CONCLUSION

The formation of spiral superstructures of PLGA amyloid fibrils coincides with a strong enhancement of their VCD intensity and the appearance of an unusual amide I band, which is likely to reflect presence of bifurcated hydrogen-bond linking (via glutamate side chains) adjacent, stacked β-sheets. Several theoretical works have accentuated the relationship between twisting of β-sheets and the increasing of VCD intensity.[13,14] We propose that the continuous arrangement of β-strands within the spiral entities visible in electron microscopy stabilize twisted and densely compressed β-sheets, through which the superstructure acquires its remarkable optical properties. We have shown that the induction of packing defects through the mixing of PLGA and PDGA does not lead to amorphous aggregates, but rather to formation of fibrils which are incapable of merging into higher-order structures.

ASSOCIATED CONTENT

Supporting Information. Additional VCD data, SEC analysis of PLGA, and acknowledgment for TEM support and assistance. This material is available free of charge via the Internet at http://pubs.acs.org.

AUTHOR INFORMATION

Corresponding Author

*Phone: +48 22 8220211 ext. 528; fax: +48 22 822 5996; e-mail: wdzwolak@chem.uw.edu.pl. Phone: +1 312 9963 156; fax: +1 312 9960 431; e-mail: tak@uic.edu.

ACKNOWLEDGMENT

We are grateful to Mr. Adam Presz for his kind help with SEM measurements and to Ms. Ge Zhang for help with the FTIR of the mixed aggregates. This work was supported by the Polish Ministry of Education and Science (grant NN 301 101236 to WD) and in part by a grant from the National Science Foundation (CHE07-19543, to TAK).

ABBREVIATIONS

AFM, atomic force microscopy; FT-IR, Fourier transform infrared; HB, hydrogen bond; MW, molecular weight; PDGA, poly(D-glutamic) acid; PLGA, poly(L-glutamic) acid; SEC, size exclusion chromatography; SEM, scanning electron microscopy; TEM, transmission electron microscopy; ThT, thioflavin T; VCD, vibrational circular dichroism

REFERENCES

(1) Chiti, F.; Dobson, C. M. *Annu. Rev. Biochem.* **2006**, *75*, 333–366.
(2) Nelson, R.; Sawaya, M. R.; Balbirnie, M.; Madsen, A. Ø.; Riekel, C.; Grothe, R.; Eisenberg, D. *Nature* **2005**, *435*, 773–778.
(3) Petkova, A. T.; Ishii, Y.; Balbach, J. J.; Antzutkin, O. N.; Leapman, R. D.; Delaglio, F.; Tycko, R. *Proc. Natl. Acad. Sci. U.S.A.* **2002**, *99*, 16742–16747.
(4) Dzwolak, W.; Loksztejn, A.; Galinska-Rakoczy, A.; Adachi, R.; Goto, Y.; Rupnicki, L. *J. Am. Chem. Soc.* **2007**, *129*, 7517–7522.
(5) Loksztejn, A.; Dzwolak, W. *J. Mol. Biol.* **2008**, *379*, 9–16.
(6) Ma, S.; Cao, X.; Mak, M.; Sadik, A.; Walkner, C.; Freedman, T. B.; Lednev, I. K.; Dukor, R. K.; Nafie, L. A. *J. Am. Chem. Soc.* **2007**, *129*, 12364–12365.
(7) Kurouski, D.; Lombardi, R. A.; Dukor, R. K.; Lednev, I. K.; Nafie, L. A. *Chem. Commun.* **2010**, *46*, 7154–7156.
(8) Fändrich, M.; Dobson, C. M. *EMBO J.* **2002**, *21*, 5682–5690.
(9) Itoh, K.; Foxman, B. M.; Fasman, G. D. *Biopolymers* **1976**, *15*, 419–455.
(10) Fulara, A.; Dzwolak, W. *J. Phys. Chem. B* **2010**, *114*, 8278–8283.
(11) Keiderling, T. A. *Curr. Opin. Chem. Biol.* **2002**, *6*, 682–688.
(12) Narayanan, U.; Keiderling, T. A.; Bonora, G. M.; Toniolo, C. *J. Am. Chem. Soc.* **1986**, *108*, 2431–2437.
(13) Kubelka, J.; Keiderling, T. A. *J. Am. Chem. Soc.* **2001**, *123*, 12048–12058.
(14) Measey, T. J.; Schweitzer-Stenner, R. *J. Am. Chem. Soc.* **2011**, *133*, 1066–1076.
(15) Dzwolak, W.; Muraki, T.; Kato, M.; Taniguchi, Y. *Biopolymers* **2004**, *73*, 463–469.
(16) Dzwolak, W.; Loksztejn, A.; Smirnovas, V. *Biochemistry* **2006**, *45*, 8143–8151.
(17) Lakhani, A.; Malon, P.; Keiderling, T. A. *Appl. Spectrosc.* **2009**, *63*, 775–785.
(18) Bour, P.; Keiderling, T. A. *J. Mol. Struct.: THEOCHEM* **2004**, *675*, 95–105.
(19) Bour, P.; Keiderling, T. A. *J. Phys. Chem. B* **2005**, *109*, 5348–5357.
(20) Dzwolak, W.; Ravindra, R.; Nicolini, C.; Jansen, R.; Winter, R. *J. Am. Chem. Soc.* **2004**, *126*, 3762–3768.
(21) Itoh, K.; Tokumi, S.; Kimura, T.; Nagase, A. *Langmuir* **2008**, *24*, 13426–13433.
(22) Sulatskaya, A. I.; Maskevich, A. A.; Kuznetsova, I. M.; Uversky, V. N.; Turoverov, K. K. *PLoS ONE* **2010**, *5*, e15385.
(23) Groenning, M. *J. Chem. Biol.* **2010**, *3*, 1–18.
(24) Dzwolak, W.; Pecul, M. *FEBS Lett.* **2005**, *579*, 6601–6603.
(25) Kodali, R.; Wetzel, R. *Curr. Opin. Struct. Biol.* **2007**, *17*, 48–57.
(26) Krejtschi, C.; Hauser, K. *Eur. Biophys. J.* **2011**No. DOI: 10.1007/s00249-011-0673-8.
(27) Krimm, S.; Bandekar, J. *Adv. Protein Chem.* **1986**, *38*, 181–364.